

# We are IntechOpen, the world's leading publisher of Open Access books Built by scientists, for scientists

4,800

Open access books available

122,000

International authors and editors

135M

Downloads

Our authors are among the

154

Countries delivered to

TOP 1%

most cited scientists

12.2%

Contributors from top 500 universities



WEB OF SCIENCE™

Selection of our books indexed in the Book Citation Index  
in Web of Science™ Core Collection (BKCI)

Interested in publishing with us?  
Contact [book.department@intechopen.com](mailto:book.department@intechopen.com)

Numbers displayed above are based on latest data collected.  
For more information visit [www.intechopen.com](http://www.intechopen.com)



# Energy-Efficient Standalone Fossil-Fuel Based Hybrid Power Systems Employing Renewable Energy Sources

R. W. Wies, R. A. Johnson and A. N. Agrawal  
*University of Alaska Fairbanks*  
USA

## 1. Introduction

The cost and efficiency of fossil fuel based electric power and heat production in remote areas is an important topic, such as in Alaska with more than 250 remote villages, and developing countries such as Mexico, with approximately 85,000 villages, each with populations less than 1000 persons. The operating cost of fossil fuel based generators such as diesel electric generators (DEGs) is primarily influenced by the cost associated with the purchase, transportation, and storage of diesel fuel. It is very expensive to transport fuel for DEGs in some villages of Alaska (Denali Commission, 2003) due to the extreme remoteness of the site. Furthermore, there are issues associated with oil spills and storage of fuels (Drouhillet & Shirazi, 1997). As of the year 2010, the average subsidized cost of electricity (COE) for a remote Alaskan community is about 0.53 USD/kWh for the first 500 kWh per residential customer per month. The unsubsidized COEs are as high as 2.00 USD/kWh for some extremely isolated communities (Denali Commission, 2003). An extension of the main grid is not possible for such communities due to high cost and losses for the transmission lines.

Based on energy consumption studies compiled by the US Department of Energy, Alaska spends about 50% more (28.71 USD per million BTU) for electrical energy than the rest of the United States (19.37 USD per million BTU) (EIA, 2002). A Memorandum of Agreement (MOA) was signed between the Denali Commission, the Alaska Energy Authority, and the Regulatory Commission of Alaska to supply reliable and reasonably priced electricity to the rural communities of Alaska (Denali Commission, 2003). With the rising cost of fuel and the need for more efficient systems with higher reliability and lower emissions, integrating renewable energy sources and energy storage devices could prove to be more cost effective solutions for electrical power in remote communities (Fyfe, Powell, Hart, & Ratanasthien, 1993). Consequently, there is great need for energy-efficient standalone smart micro-grid systems in these remote communities that employ renewable power sources and energy storage devices.

Distributed power generation systems consisting of two or more generation and storage components, including solar PV arrays, WTGs, battery banks, DEGs, and microhydro, are widely used to supply energy needs. Renewable energy sources such as solar photovoltaics (PV) and wind turbine generators (WTGs) could be used in conjunction with DEGs to supply

electricity in remote Alaskan communities and other remote regions (Denali Commission, 2003), (Drouhillet & Shirazi, 1997), (Dawson & Dewan, 1989), (Wies, et al., 2005a), (Wies, et al., 2005b), (Wies, et al., 2005c), & (Borowy, 1996). Besides reducing fuel consumption, the use of renewable energy sources has been shown to increase system efficiency and reliability, while reducing emissions (Drouhillet & Shirazi, 1997), (Dawson & Dewan, 1989), (Wies, et al., 2005a), (Wies, et al., 2005b), (Wies, et al., 2005c), & (Borowy, 1996). It has been predicted that by the year 2050, despite the increase in the demand for electric power, the global CO<sub>2</sub> level which is the major greenhouse gas would be reduced to 75% of its 1985 level due to the increase in the use of renewable energy sources for energy production (Johansson, et al., 1993).

This remainder of this chapter presents an economic and environmental model for standalone fossil fuel based micro-grid systems employing renewable energy sources based on an existing diesel-electric power generation systems in remote arctic communities. A simulator called the Hybrid Arctic Remote Power Simulator (HARPSim) was developed using MATLAB<sup>®</sup> Simulink<sup>®</sup> to estimate the reduction in fuel consumption of DEGs and the minimization in the cost of producing electricity in remote locations by integrating solar PV and WTGs into the system. HARPSim is used to predict the long-term economic and environmental performance of the system with and without the use of renewable sources in combination with the diesel electric power generation system. A battery bank is also included in the system to serve as a backup and a buffer/storage interface between the DEGs and the variable sources of power from solar PV and wind.

The economic part of the model calculates the fuel consumed, the kilowatt-hours (kWhrs) obtained per liter (gallon) of fuel supplied, and the total cost of fuel. The environmental part of the model calculates the CO<sub>2</sub>, particulate matter (PM), and the NO<sub>x</sub> emitted to the atmosphere. The Life Cycle Cost (LCC), net present value (NPV), efficiency, and air emissions results of the Simulink<sup>®</sup> model are compared with those predicted by the Hybrid Optimization Model for Electric Renewables (HOMER) software developed at the National Renewable Energy Laboratory (NREL) (NREL HOMER, 2007). A sensitivity analysis of fuel cost and investment rate on the COE is also performed to illustrate the impact of rising fuel costs on the long-term system economics.

## 2. Distributed generation system

Distributed generation systems like the one described here are currently used in many parts of the world. While this work focuses on modeling a distributed electric power generation system for the remote arctic community in Alaska, the general model can be applied to any distributed generation system containing these components, but can also be extended to include other energy technologies.

### 2.1 General block diagram

A simple block diagram of a standalone distributed (hybrid) power system is shown in Fig. 1. The sources of electric power in this system consist of a DEG, a battery bank, a WTG, and a PV array. The output of the diesel generator is regulated AC voltage, which supplies the load directly through the main distribution transformer. The connection of the battery bank, the WTG, and the PV array are through a DC bus. The control unit regulates the flow of power to and/or from the sources, depending on the load. The load in the hybrid power system can be an AC load, a DC load, a heating load (resistive load bank), or a hybrid load.

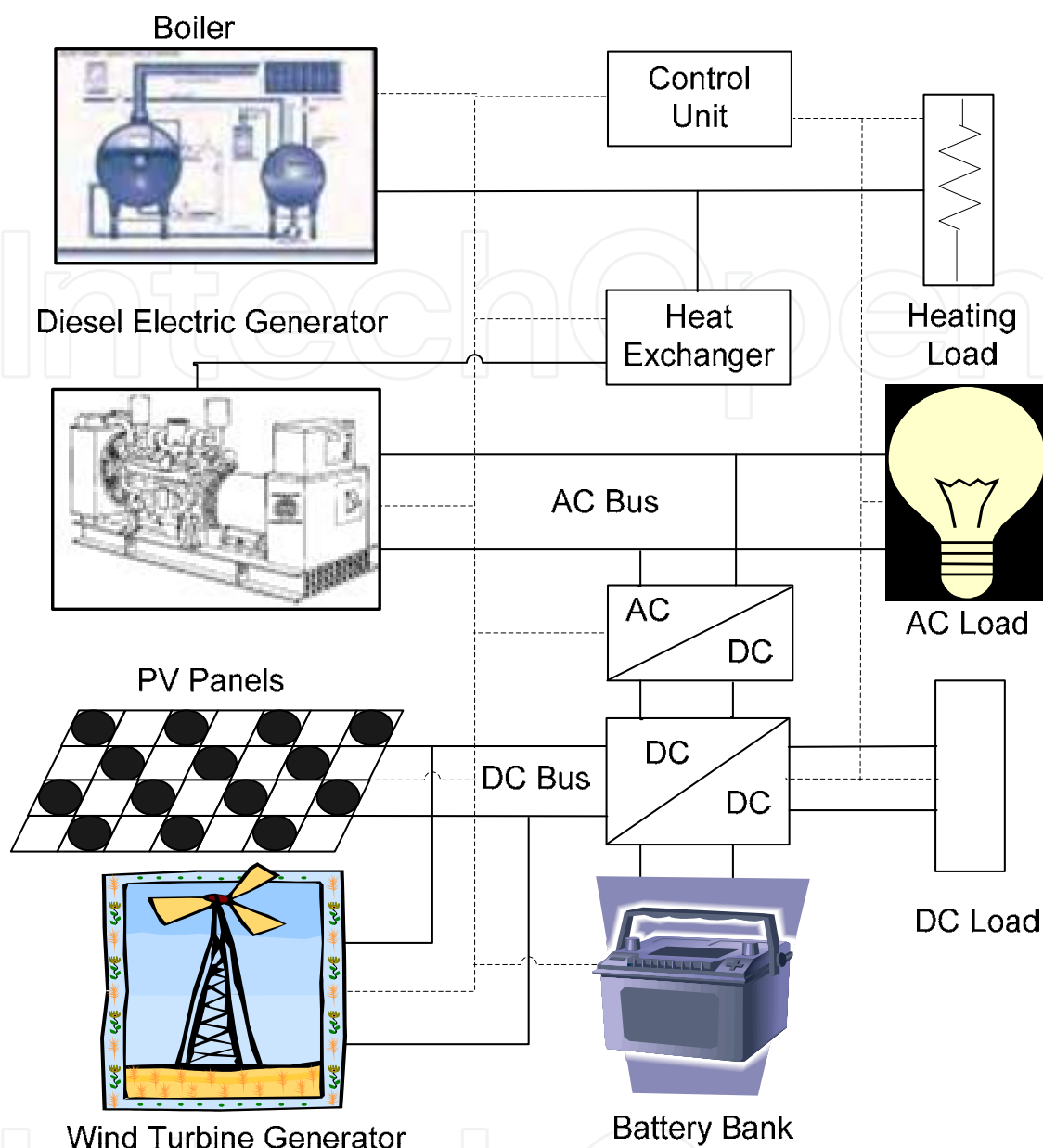


Fig. 1. General distributed (hybrid) power generation system.

## 2.2 Sample standalone village power system

The sample standalone distributed (hybrid) electric power system used in this analysis consists of four DEGs rated at 235 kW, 190 kW, 190 kW, and 140 kW. The average electrical load is 95 kW with a minimum of 45 kW and a maximum of 150 kW. One DEG is sufficient to supply the village load. Currently, a PV array and a WTG are not installed in the system. In order to analyze the long-term performance of the system while integrating a PV array, a WTG, and a battery bank, simulations were performed using HARPSim for a PV-diesel-battery system, a wind-diesel-battery system, and a PV-wind-diesel-battery system. The simulation results were compared with those predicted by the HOMER software. The system performance is analyzed by incorporating a 100 kWh absolute IIP battery bank, a 12 kW PV array, a 65 kW 15/50 AOC WTG, and a 100 kVA bi-directional power converter.

### 3. Simulation model

A general model block diagram for the wind-PV-diesel-battery hybrid power system is shown in Fig. 2. The model is based on previous work with a PV-diesel-battery system (Wies, et al., 2005a) & (Wies, et al., 2005b), and a wind-diesel battery system (Wies, et al., 2005c). The basic model blocks in Fig. 2 and their subsystems are described in detail in Chapter 2 of (Agrawal, 2006). The model consists of nine different subsystems contained in blocks. The electrical energy sources in the model include DEGs, subsystems are described in detail in Chapter 2 of (Agrawal, 2006). The model consists of nine different subsystems contained in blocks. The electrical energy sources in the model include DEGs, WTGs, a PV array, and a battery bank. Currently, the Simulink® model performs a long term performance analysis including the environmental impact calculations of the hybrid power system under consideration. The different inputs required include the annual load and power factor profile, the annual wind speed for the WTGs, the annual insolation profile for the PV array, the annual ambient air temperature in which the power system is operating, the kW ratings of the generators, and the kW rating of the battery bank.

Some basic information about the DEG, Fuel Consumption, Wind, PV, and Battery subsystem models are provided in the following sections.

#### 3.1 DEG and fuel consumption model

The DEG consists of two parts: the electric generator and the diesel engine. The electric generator model consists of the efficiency curve that describes the relationship between the electrical efficiency and the electrical load on the generator. Fig. 3 shows a typical electrical efficiency curve for an electric generator. The fuel curve for a diesel engine describes the amount of fuel consumed depending on the engine load. A typical diesel engine fuel curve is a linear plot of load versus fuel consumption as shown in Fig. 4.

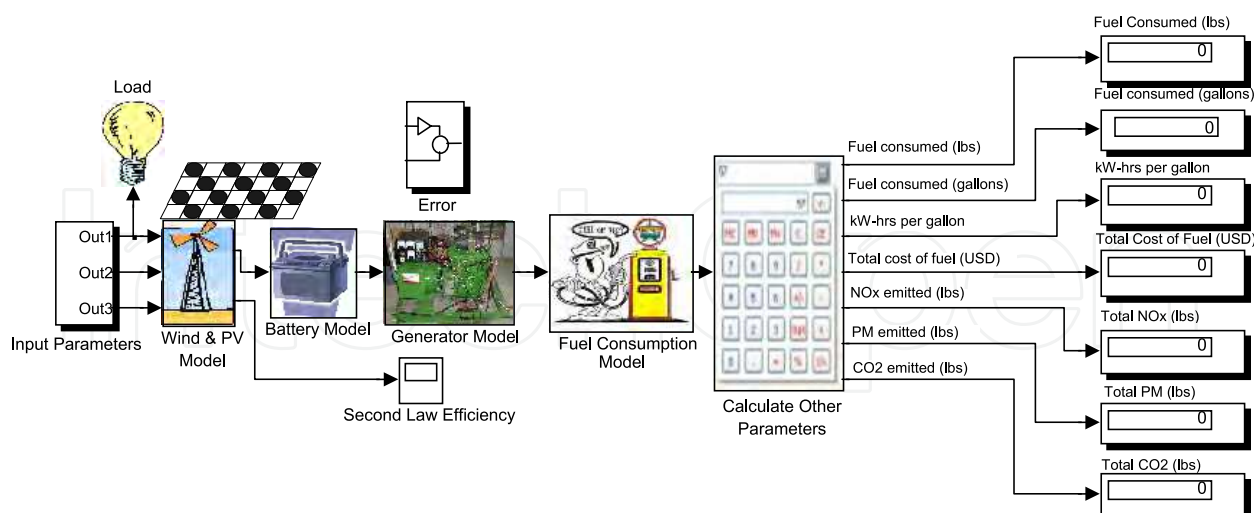


Fig. 2. PV-wind-diesel-battery hybrid power system model.

A fourth order polynomial fit for the electrical efficiency curve as a function of the generator electrical load ' $L_{gen}$ ' at unity ' $\eta_{e1}$ ' and 0.8 ' $\eta_{e2}$ ' power factor is used. The actual load on the electric generator is converted to its percentage value by dividing the actual load by the electric generator rating and multiplying by 100. This operation is performed so that the

same efficiency equations are independent of the rating of the electric generators. The values for the electrical efficiency  $\eta_{el}$  of the generator and the mechanical load 'L<sub>eng</sub>' on the engine for any given power factor 'pf' are determined using linear interpolation as follows:

$$\eta_{el} = \eta_{el2} + \left( \frac{(\eta_{el1} - \eta_{el2}) * (pf - 0.8)}{0.2} \right) \tag{1}$$

$$L_{eng} = \frac{L_{gen}}{\eta_{el}} \tag{2}$$

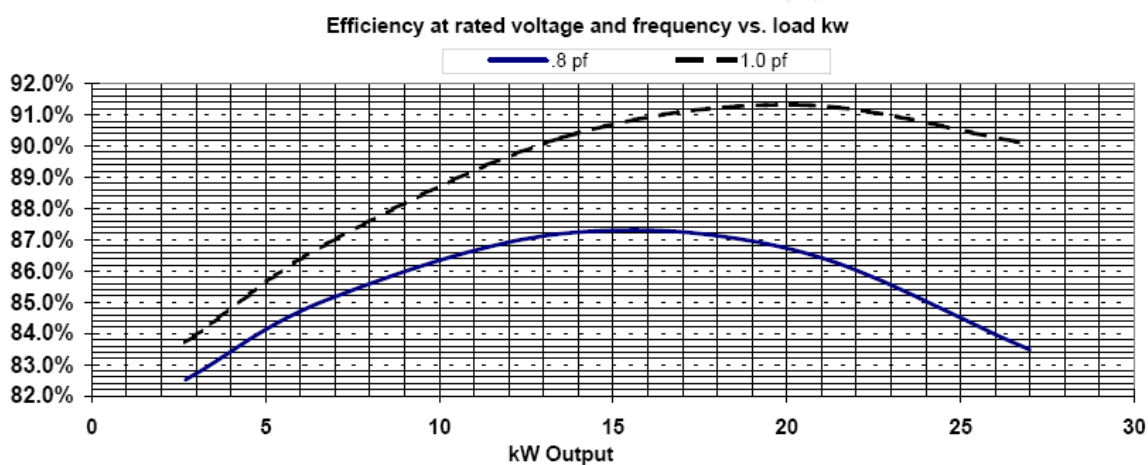


Fig. 3. Typical efficiency for an electric generator.

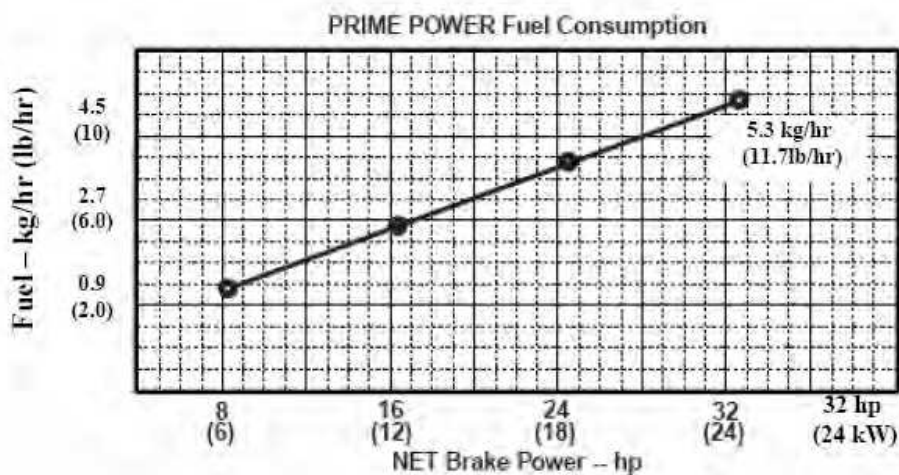


Fig. 4. Typical fuel consumption curve for DEG.

The linear fit for the diesel engine fuel curve is given as

$$\dot{F}_c = 0.5 * \left( L_{eng} * \frac{kW - A}{100} \right) - 0.44 \tag{3}$$

and

$$\text{Total } F_c = \int_0^T \dot{F}_c .dt \quad (4)$$

where ' $\dot{F}_c$ ' is the fuel consumption rate in kg/hr (lbs/hr), ' $L_{eng}$ ' is the percentage load on the engine, ' $kW_A$ ' is the rating of the electric generator, ' $F_c$ ' is the total fuel consumed in kg (lbs), ' $dt$ ' is the simulation time-step, and ' $T$ ' is the simulation period. The fuel consumed in kg (lbs) is obtained by multiplying the fuel consumption rate of kg/hr (lbs/hr) by the simulation time-step ' $dt$ ' (given in hours), and the total fuel consumption in kg (lbs) is obtained by integrating the term ' $\dot{F}_c dt$ ' over the period of the simulation.

When two or more DEGs supply the load, it is important that the DEGs operate optimally. The following steps are performed to find the optimal point of operation for DEG 2.

1. The electrical generator (Fig. 3) and diesel engine (Fig. 4) performance curves are used to determine overall fuel consumption for the given load profile.
2. The load on the DEGs is varied from 0 to 100%.
3. The fuel consumption for each DEG is noted at different load points.
4. The point of intersection of the two curves is the optimal point of operation for DEG 2. Beyond this point DEG 1 is more efficient than DEG 2.
5. If the two curves do not intersect, the optimal point is taken as 0. This situation implies that DEG 1 is efficient throughout the operating range of the load.

Fig. 5 shows the overall fuel consumption curves for the two DEGs and the optimal point of operation for DEG 2. In order to avoid premature mechanical failures, it is important that DEGs operate above a particular load (generally 40% of rated). The long-term operation of DEGs at light loads leads to hydrocarbon built-up in the engine, resulting in high maintenance cost and reduced engine life (Malosh & Johnson, 1985). If the optimal point is less than 40% load, it is adjusted so that DEG 2 operates at or over 40% load.

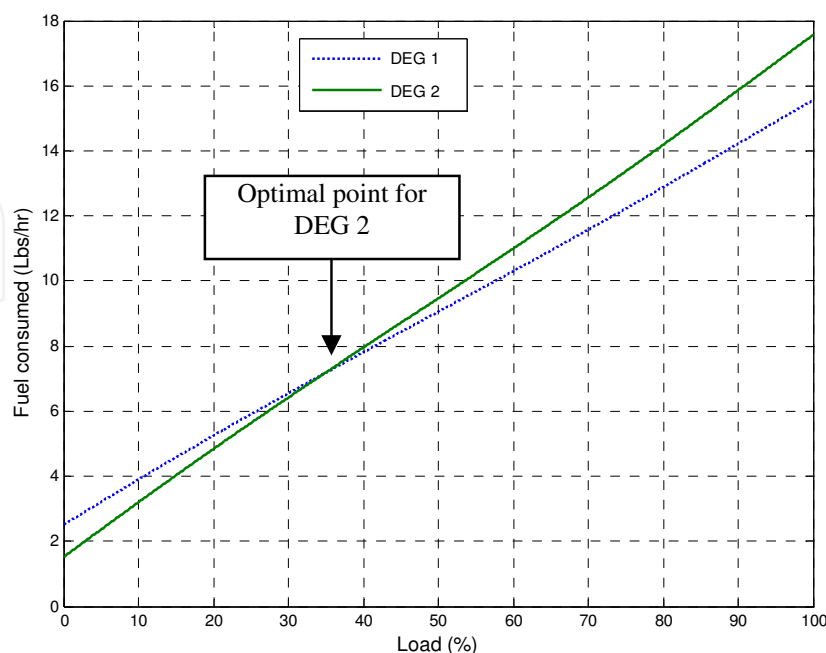


Fig. 5. Optimal point of operation for DEG 2.

### 3.2 Wind model

The *Wind Model* block calculates the total power available from the wind turbines based on the power curve. The power curve gives the value of the electrical power based on the wind speed. The wind turbine used in this simulation is the 15/50 Atlantic Orient Corporation (AOC). Fig. 6 shows the power curve for the 15/50 AOC wind turbine generator (AOC, 2007). This block calculates the power available from the WTGs depending on the speed of wind based on a look-up table (Table 1).

The wind model block also calculates the second law efficiency of the WTG. The second law efficiency of the WTG is given as

$$\eta_{\text{second law}} = \frac{\text{actual power}}{\text{max possible power}} \quad (5)$$

where ' $\eta_{\text{second law}}$ ' is the second law efficiency of the WTG, 'actual\_power' is the actual power output from the WTG and 'max\_possible\_power' is the maximum possible power output from the WTG.

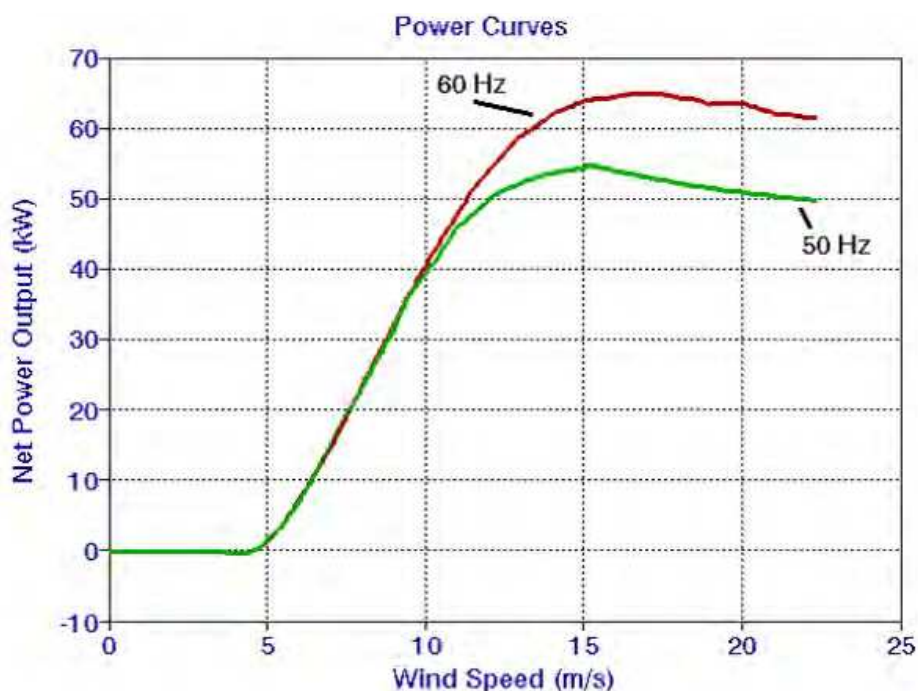


Fig. 6. Power curve for 15/50 Atlantic Oriental Corporation WTG [13].

The actual power of the wind turbine is obtained from the manufacturer's power curve and the maximum possible power is obtained from the Betz formula described in (Patel, 1999) as

$$P_{max} = \frac{1}{2} \rho A V^3 \times (0.59) P_{max} \quad (6)$$

where ' $P_{max}$ ' is the maximum possible power, ' $\rho$ ' is the density of air taken as 1.225 kg/m<sup>3</sup> (0.076 lb/ft<sup>3</sup>) at sea level, 1 atmospheric pressure i.e. 101.325 kPa (14.7 psi), and a temperature of 15.55°C (60°F), ' $A$ ' is the rotor swept area in m<sup>2</sup> (ft<sup>2</sup>), ' $V$ ' is the velocity of wind in m/s (miles/hour), and the factor '0.59' is the theoretical maximum value of power

coefficient of the rotor ( $C_p$ ) or theoretical maximum rotor efficiency which is the fraction of the upstream wind power that is captured by the rotor blade. It should be noted from (6) that the wind power varies with the cube of the air velocity. Therefore, a slight change in wind speed results in a large change in the wind power.

Sr. No.	Wind speed		Net power output (kW)
	Meters/second	Miles/hour	
1	0	0	0
2	5	11.18468	2
3	10	22.37	40
4	11.5	25.725	50
5	13.5	30.1986	60
6	15	33.554	63
7	17	38.028	65
8	19	42.5	63
9	21	46.975	62
10	22.5	50.331	61

Table 1. Look-Up Table for the 15/50 AOC Wind Turbines

The air density ' $\rho$ ' can be corrected for the site specific temperature and pressure in accordance with the gas law

$$\rho = \frac{p}{RT} \quad (7)$$

where ' $\rho$ ' is the density of air, ' $p$ ' is the air pressure, ' $R$ ' is the gas constant, and ' $T$ ' is the temperature.

### 3.3 PV model

The PV model block calculates the PV power (kW) and the total PV energy (kWh) supplied by the PV array using the following equations.

$$P_{PV} = \eta_{pv} * ins * A * PV \quad (8)$$

and

$$E_{PV} = \int_0^T P_{PV} \cdot dt, \quad (9)$$

where ' $P_{PV}$ ' is the power obtained from the PV array (kW), ' $\eta_{pv}$ ' is the efficiency of the solar collector, ' $ins$ ' is the solar insolation (kWh/m<sup>2</sup>/day), ' $A$ ' is the area of the solar collector/kW, ' $PV$ ' is the rating of the PV array (kW), and  $E_{PV}$  is the total energy obtained from the PV array.

The efficiency of the solar collector is obtained from the manufacturer. The data sheets for the solar panels manufactured by Siemens and BP are available in Appendix 4 of (Agrawal, 2006). The solar insolation values are available from the site data or can be obtained by using the solar maps from the National Renewable Energy Laboratory website (NREL GIS Solar Maps, 2007). The area of the solar collector depends on the number of PV modules and the dimensions of each module. The number of PV modules depends on the installed capacity of the PV array and the dimensions of each PV module are obtained from the manufacturer's data sheet.

### 3.4 Battery model

In the Simulink® model, the battery bank is modeled so that it acts as a source of power, rather than back-up power. The battery model block controls the flow of power to and from the battery bank. A roundtrip efficiency of 90% is assumed for the battery charge and discharge cycle. The battery model incorporates the effect of ambient temperature as described in (Winsor & Butt, 1978) into the hybrid power system model. Therefore, the model can be used for cold region applications.

The life of the battery bank depends on the depth of discharge and the number of charge discharge cycles. In the Simulink® model the battery bank is modeled so that it acts as a source of power rather than back-up power. Therefore, the depth of discharge of the battery-bank is assumed between 95% and 20% of the rated capacity. This higher depth of discharge reduces the number of battery operating cycles for the same energy output. It should be noted that the number of battery cycles plays a more significant role in the life of the battery bank.

### 3.5 Fuel consumption and emissions

The *Calculate Other Parameters* block calculates parameters like the total kWhrs/gallon supplied by the generator, the fuel consumed in lbs, the fuel consumed in gallons, the total cost of fuel in USD, the amount of CO<sub>2</sub> emissions, the amount of particulate matter (PM<sub>10</sub>) emissions, and the amount of NO<sub>x</sub> emissions. For example, the kWhrs/gallon supplied by the generator and the total cost of fuel in USD are calculated as

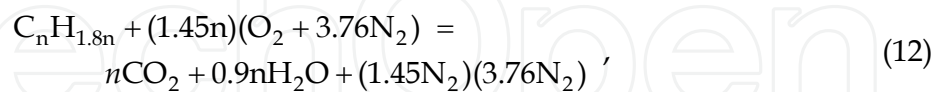
$$\text{kWhrs/gallon} = \frac{\text{kWhr}_{\text{Gen}}}{F_C} \quad (10)$$

and

$$\text{Total cost (USD)} = F_C \cdot \text{cost/gallon}, \quad (11)$$

where  $\text{kWhr}_{\text{Gen}}$  is the total kWhr supplied by the diesel generator and  $F_C$  is the total fuel consumed in gallons. The quantity cost/gallon is the cost of fuel (USD) per gallon and varies for different locations.

The total  $\text{CO}_2$  emissions were estimated based on the equation for the combustion of diesel fuel. For example, one empirical formula for light diesel  $\text{C}_n\text{H}_{1.8n}$  is given in (Cengel & Boles, 2002). For this empirical formula, with 0 % excess air the combustion reaction is given as



where  $n$  is the number of atoms. For any  $n$ , the mass in kg (lb) of  $\text{CO}_2$  per unit mass in kg (lb) of fuel =  $44/(12 + 1.8) = 3.19$ . For example, to get the emissions per unit electrical energy output, the above is combined with an engine efficiency of 3.17 kWh/liter (12 kWhr/gallon) and a fuel density of 0.804 kg/liter (6.7 lb/gallon). Doing this results in specific  $\text{CO}_2$  emissions of  $3.1*(0.804/3.17) = 0.786$  kg (1.73 lb) of  $\text{CO}_2$  per kWh of electricity which agrees closely with 0.794 kg/kWh (1.75 lb/kWh) obtained from the DEG manufacturer.

The annual  $\text{CO}_2$  amount was calculated from the lb  $\text{CO}_2/\text{kWh}$  and the annual kWh produced and is given as follows:

$$\text{Total pollutant in kg (lb)} = \frac{\text{pollutant}}{\text{kWh}} * \text{kWh}_{\text{Gen}}, \quad (13)$$

where  $\text{kWh}_{\text{Gen}}$  is the total kWh supplied by the diesel generator during the simulation period. The corresponding values for  $\text{PM}_{10}$  and  $\text{NO}_x$  emissions can be obtained from the manufacturer using relations similar to (13).

### 3.6 Overall model operation and algorithm flow

Fig. 7 shows the algorithm flow chart for the PV-wind-diesel-battery hybrid power system. In the PV-wind-diesel-battery system, the PV array and the WTGs have the highest priority to supply the load. If the load is not met by the PV array and WTGs, the battery bank is used to supply the required load, and if the battery bank is less than 20% charged, the controller sends a signal to the diesel generator to turn "on" and the diesel generator is then used to supply the desired load and charge the batteries at the same time. On the other hand if there is excess power available from the PV array and WTGs, the excess power is sent to a resistive/dump load which can be used for space heating purposes. It should be noted that there is a high demand for heating load during the long winter months in remote communities of Alaska.

Various output parameters from the model include: the second law efficiency of the WTGs (%), the power supplied by the WTGs (kW), the power supplied by the PV array (kW), total fuel consumed in liters (gallons), total fuel cost (USD), total  $\text{CO}_2$  emitted (metric tons), total  $\text{NO}_x$  emitted in kg (pounds), and total  $\text{PM}_{10}$  emitted in kg (pounds). These output parameters are used to calculate the life cycle cost (LCC) and net present value (NPV), the cost of electricity (COE), the payback period for the PV array and the WTGs, and the avoided cost of pollutants.

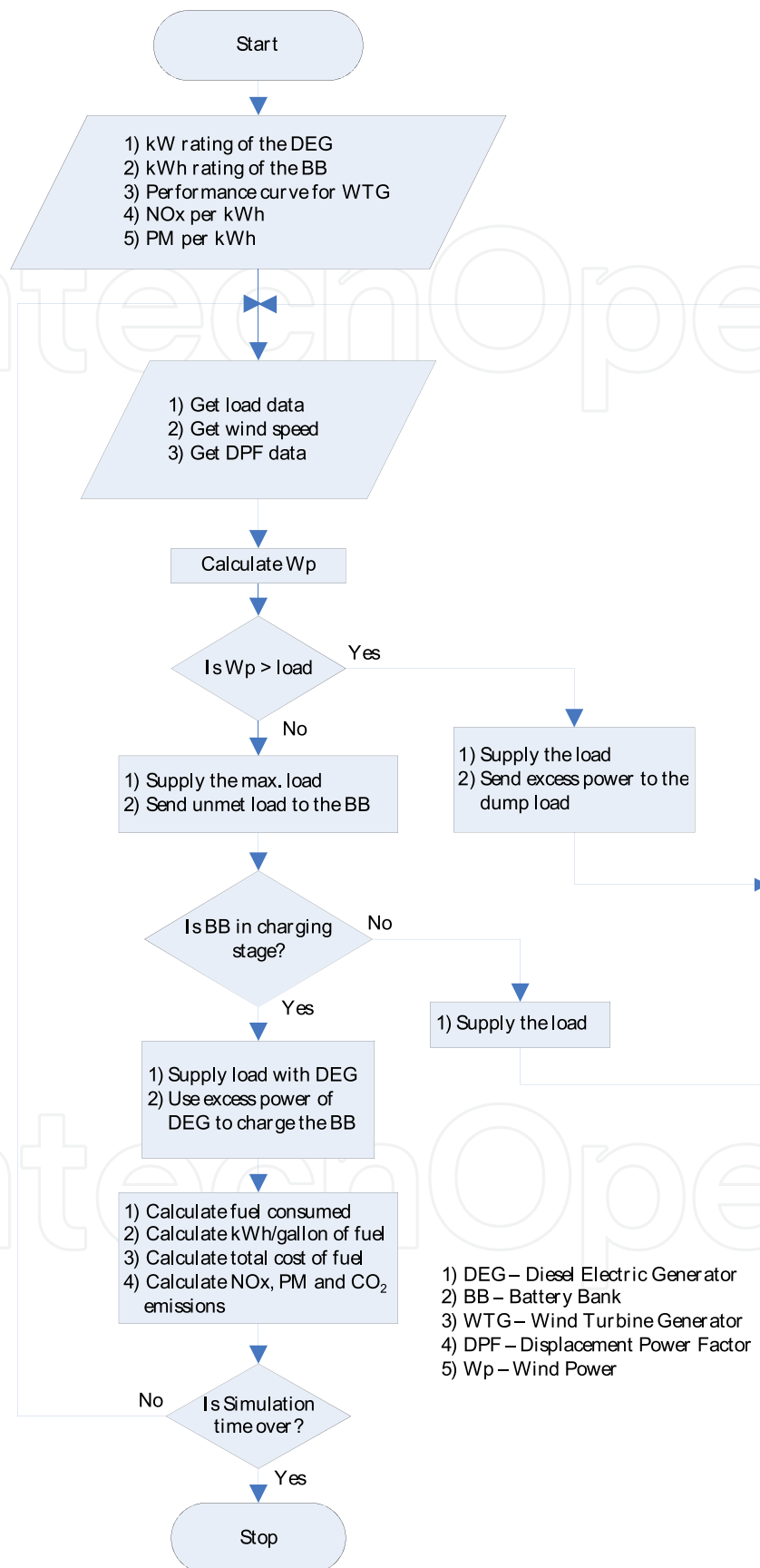


Fig. 7. Flow chart for model algorithm.

## 4. Simulation cases, results and discussion

### 4.1 System load, wind, and solar flux profile

The annual synthetic load profile from January 1<sup>st</sup>, 2003 to December 31<sup>st</sup>, 2003 with one hour average samples, the annual synthetic wind speed profile, and the annual solar flux profile used for analyzing the performance of a sample village power system are shown in Fig. 8, Fig. 9, and Fig. 10, respectively. It can be observed from Fig. 8 that the maximum load

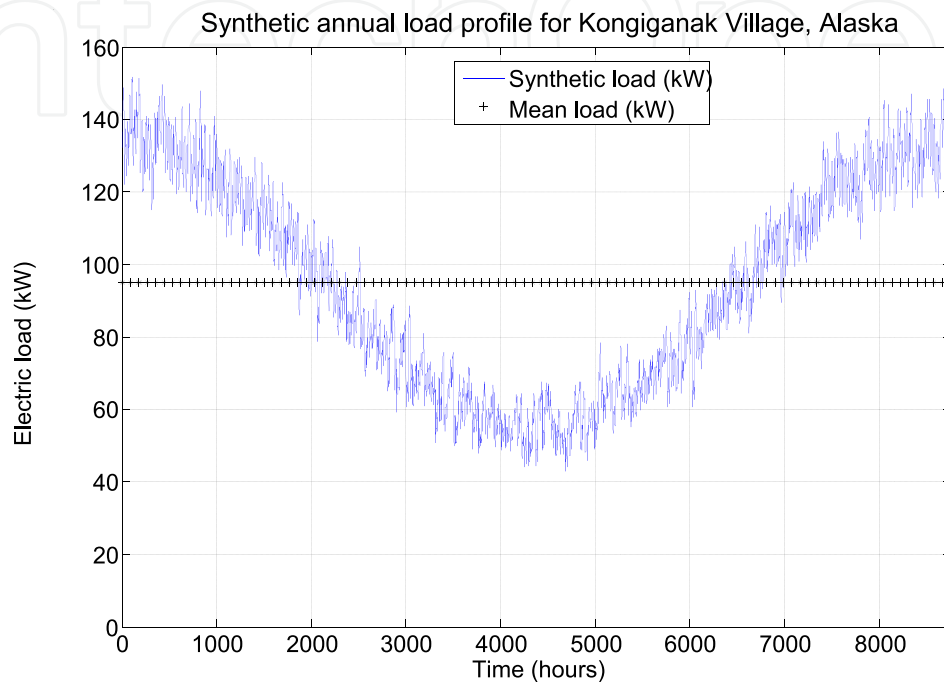


Fig. 8. Synthetic annual load profile for sample village electric power system.

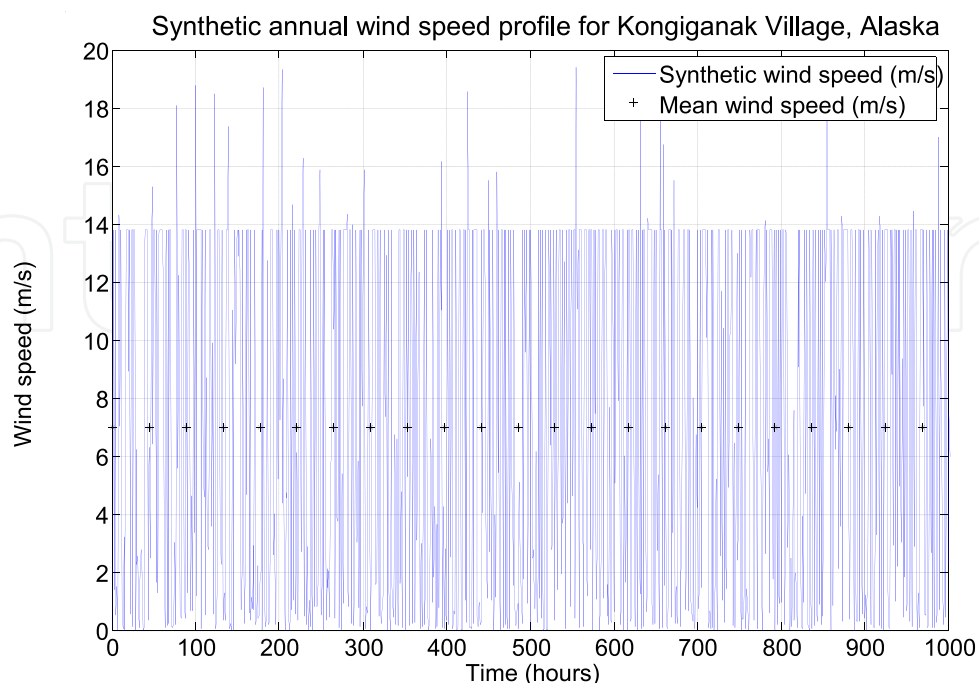


Fig. 9. Synthetic annual wind speed profile for Kongiganak Village, Alaska.

of the system is about 150 kW, the minimum load is about 45 kW and the average load is about 95 kW. From Fig. 9 it can be observed that the annual average wind speed is about 7 m/s (15.66 miles/hr). From Fig. 01 it can be observed that the village has low solar flux during winter months and high solar flux during summer months. The clearness index data for the solar insolation profile is obtained using the solar maps developed by NREL (NREL Solar Radiation Resource, 2007).

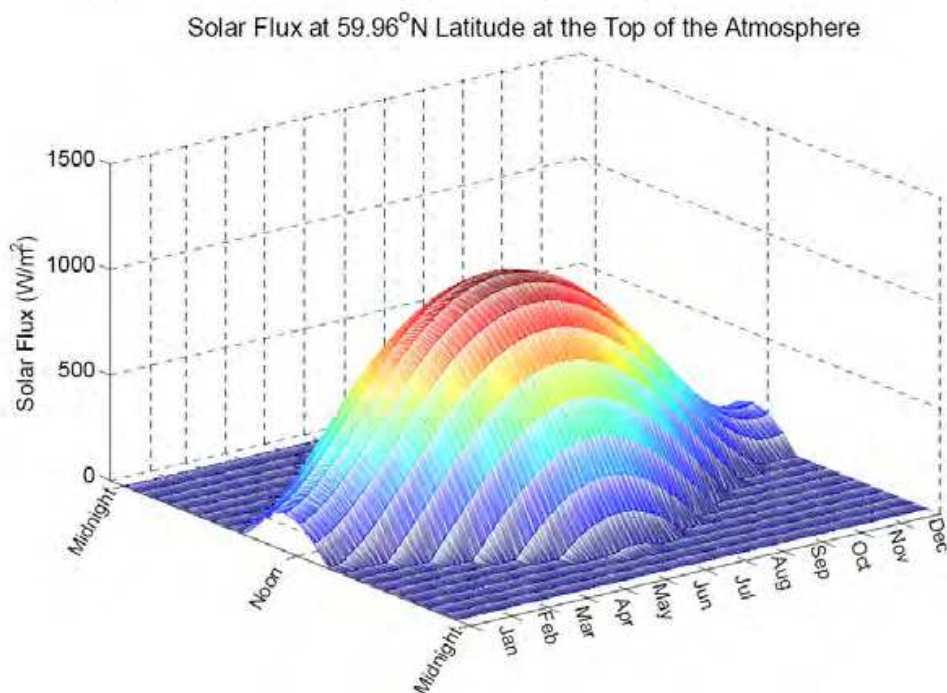


Fig. 10. Annual solar flux for Kongiganak Village, Alaska.

#### 4.2 Simulation cases and results

Simulations were performed for the standalone hybrid power system using the annual load profile for four systems: (i) diesel-battery system, (ii) PV-diesel-battery system, (iii) wind-diesel-battery system, and (iv) PV-wind-diesel-battery system.

The following assumptions were used for the Kongiganak Village simulations:

1. Interest rate  $i = 7\%$ .
2. Fuel cost of 0.80 USD/liter (3.00 USD/gallon).
3. Life cycle period for PV and WTG ( $n$ ) = 20 years.
4. Life cycle period for diesel-battery system = 5 years.
5. Life cycle period for diesel-battery system when operating with PV and WTG = 5.5 years.

Table 2 shows the installation costs (USD) for different components for the hybrid electric power system. The post simulation results obtained from the HARPSim model were compared with those obtained from the HOMER software. Table 3 shows the comparison of results from the HARPSim model with HOMER for the hybrid electric power system. It can be observed from the table that the wind-diesel-battery system is the most cost effective system with the lowest NPV, COE, and payback period. This is because of the high energy

available from the WTG. The WTG penetration level is observed as 28%. Due to its location, the solar flux available in this region is low resulting in low energy penetration from the PV array. The payback period of the WTG is obtained a little over a year and the payback period for the PV array and the WTG for the PV-wind-diesel-battery system is obtained as a little over two years. It can also be observed that the NPV of the wind-diesel-battery system using HARPSim is less than HOMER. This is because in HARPSim the battery bank charges and discharges while supplying the load. Therefore, the DEGs operate more efficiently resulting in fuel savings while emitting less pollutant. However, this fuel savings is achieved at the expense of the battery life.

Item	Cost per unit (USD)	No of units	Diesel-only system (USD)	Diesel-battery system (USD)	PV-diesel-battery system (USD)	Wind-diesel-battery system (USD)	PV-wind-diesel-battery system (USD)	2 wind-diesel-battery system (USD)
140 kW diesel generator	40,000	1	40,000	40,000	40,000	40,000	40,000	40,000
190 kW diesel generator	45,000	1	45,000	45,000	45,000	45,000	45,000	45,000
Switch gear to automate control of the system	16,000	1	16,000	18,000	20,000	20,000	22,000	30,000
Rectification/Inversion	18,000	1	0	18,000	18,000	18,000	18,000	28,000
New Absolyte IIP 6-90A13 battery bank	2,143	16	0	34,288	34,288	34,288	34,288	68,576
AOC 15/50 wind turbine generator	55,000	1	0	0	0	55,000	55,000	110,000
Siemens M55 solar panels	262	180	0	0	47,160	0	47,160	0
Engineering		1	3,000	3,500	4,000	4,000	4,500	6,000
Commissioning, Installation, freight, travel, miscellaneous		1	13,000	14,000	16,000	18,000	20,000	30,000
		TOTAL	117,000	172,788	224,448	234,288	285,948	357,576

Table 2. Installation Costs for Different Components.

Since the wind-diesel-battery system was observed to be the most cost effective system, further work was carried out to study the effect of installing another WTG into the wind-diesel-battery system. The addition of a second WTG required an increase in the capacity of the battery bank to accommodate more energy storage. Therefore, the battery bank capacity and the inverter rating were increased from 100 kW and 100 kVA to 200 kW and 200 kVA, respectively.

Item	Diesel-battery system		PV-diesel-battery system		Wind-diesel-battery system		PV-wind-diesel-battery system	
	HARPSim	HOMER	HARPSim	HOMER	HARPSim	HOMER	HARPSim	HOMER
System cost (USD)	172,788	172,788	224,448	224,450	234,288	234,288	285,948	285,950
Engine efficiency (%)	29.3	28.63	29.3	28.51	29.3	27.03	29.3	26.88
kWh/liter (kWh/gallon) for the engine	3.11 (11.75)	3.04 (11.48)	3.11 (11.75)	3.02 (11.43)	3.11 (11.75)	2.87 (10.84)	3.11 (11.75)	2.85 (10.78)
Fuel consumed in liters (gallons)	267,662 (70,810)	273,910 (72,463)	264,834 (70,062)	272,568 (72,108)	193,249 (51,124)	216,027 (57,150)	190,837 (50,486)	214,776 (56,819)
Total cost of fuel (USD)	212,429	217,390	210,185	216,325	153,373	171,451	151,458	170,456
Energy supplied								
(a) Diesel engine (kWh)	832,152	832,205	823,368	823,422	597,145	619,504	588,362	612,287
(b) WTG (kWh)	-	-	-	-	235,007	238,000	235,007	238,000
(c) PV array (kWh)	-	-	8,784	8,783	-	-	8,784	8,783
Energy supplied to load (kWh)	832,152	832,205	832,152	832,205	832,152	832,205	832,152	832,205
Operational life								
(a) Generator (years)	5	1.87	5	1.87	5	1.8	5	1.8
(b) Battery bank (years)	5	12	5.5	12	5.5	12	6	12
Net present value (USD) with $i = 7\%$ and $n = 20$ years	-	1,992,488	2,545,084	2,945,502	1,954,127	2,383,766	1,974,389	2,421,502
Cost of Electricity (USD/kWh)	0.301	22.6	0.304	0.334	0.237	0.27	0.24	0.275
Payback period for renewable (years)	-	-	Never	-	1.07	-	2.12	-
Emissions								
(a) CO <sub>2</sub> in metric tons (US tons)	660 (728)	703 (775)	653 (720)	700 (772)	477 (526)	555 (612)	471 (519)	552 (608)
(b) NO <sub>x</sub> in kg (lbs)	7,322 (16,143)	-	7,245 (15,972)	-	5,288 (11,657)	-	5,222 (11,512)	-
(c) PM <sub>10</sub> in kg (lbs)	308 (679)	-	305 (672)	-	222 (490)	-	220 (484)	-

Table 3. Comparison of Results from HARPSim with HOMER.

Table 4 shows the comparison of results from the HARPSim model with HOMER for the two wind-diesel-battery hybrid power system. It can be observed that the addition of the second WTG into the wind-diesel-battery hybrid power system resulted in the further reduction in the NPV and the COE, while the payback period with the two WTGs increased slightly. The WTG penetration level increases to 50% for this case. The payback period of the WTGs has increased to 1.56 years due to the extra cost involved in the addition of the second WTG.

Item	Two wind-diesel-battery system	
	HARPSim	HOMER
System cost (USD)	357,576	357,576
Engine efficiency (%)	29.3	26.6
kWh/liter (kWh/gallon) for the engine	3.11 (11.75)	2.78 (10.53)
Fuel consumed in liters (gallons)	151,252 (39,961)	201,444 (53,222)
Total cost of fuel (USD)	119,883	159,876
Energy supplied		
(a) Diesel engine (kWh)	469,542	561,741
(b) WTG (kWh)	470,015	475,999
Energy supplied to load (kWh)	832,152	832,205
Operational life		
(a) Generator (years)	5	1.8
(b) Battery bank (years)	5.5	12
Net present value (USD) with $i = 7\%$ and $n = 20$ years	1,748,988	2,407,895
Cost of Electricity (USD/kWh)	0.22	0.273
Payback period for WTG (years)	1.56	-
Emissions		
(a) CO <sub>2</sub> in metric tons (US ton)	367 (405)	517 (570)
(b) NO <sub>x</sub> in kg (lbs)	4,068 (9,112)	-
(c) PM <sub>10</sub> in kg (lbs)	171 (383)	-

Table 4. Comparison of Results from HARPSim with HOMER for Two Wind-Diesel-Battery Hybrid Power System.

### 4.3 Life cycle cost and net present value analysis

The life cycle cost (LCC) is the total cost of the system over the period of its life cycle including the cost of installation, operation, maintenance, replacement, and the fuel cost. The life cycle cost also includes the interest paid on the money borrowed from the bank or other financial institutes to start the project. The life cycle cost of the project can be calculated as follows:

$$LCC = C + M + E + R - S \quad (14)$$

where 'LCC' is the life cycle cost, 'C' is the installation cost (capital cost), 'M' is the overhead and maintenance cost, 'E' is the energy cost (fuel cost), 'R' is the replacement and repair costs, and 'S' is the salvage value of the project.

The net present value (NPV) is the money that will be spent in the future discounted to today's money. The NPV plays an important role in deciding the type of the system to be installed. The NPV of a system is used to calculate the total spending on the installation, maintenance, replacement, and fuel cost for the type of system over the life-cycle of the project. Knowing the NPV of different systems, the user can install a system with minimum NPV. The relationships used in the calculation of NPV are given as follows:

$$P = \frac{F}{(1+I)^N} \tag{15}$$

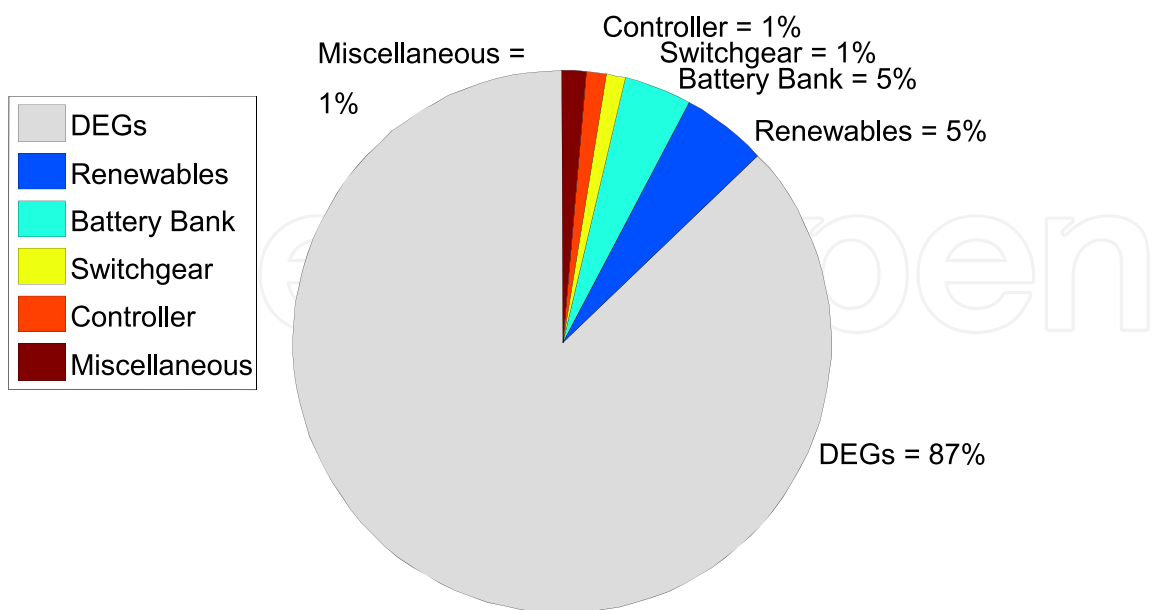
and

$$P = \frac{A[1 - (1+I)^{-N}]}{I}, \tag{16}$$

where 'P' is the present worth, 'F' is the money that will be spent in the future, 'I' is the discount rate, 'N' is the year in which the money will be spent, and 'A' is the annual sum of money.

Fig. 11 and Fig. 12 show the LCC analysis of the PV-wind-diesel-battery hybrid power system using HARPSim and HOMER, respectively. It can be seen that in HARPSim, the cost of DEGs is 4% less while the cost of the battery bank is 2% more than in HOMER. This is because in HARPSim, the battery bank acts as a source of power rather than as the backup

20-year LCC analysis of the Kongiganak Village hybrid power system using HARPSim



The NPV of the system, with  $i = 7\%$  and fuel cost = 0.79 USD per liter (3.0 USD per gallon), is 1,974,389 USD

Fig. 11. 20-year LCC analysis of the hybrid power system using HARPSim.

### 20-year LCC analysis of the Kongiganak Village hybrid power system using HOMER

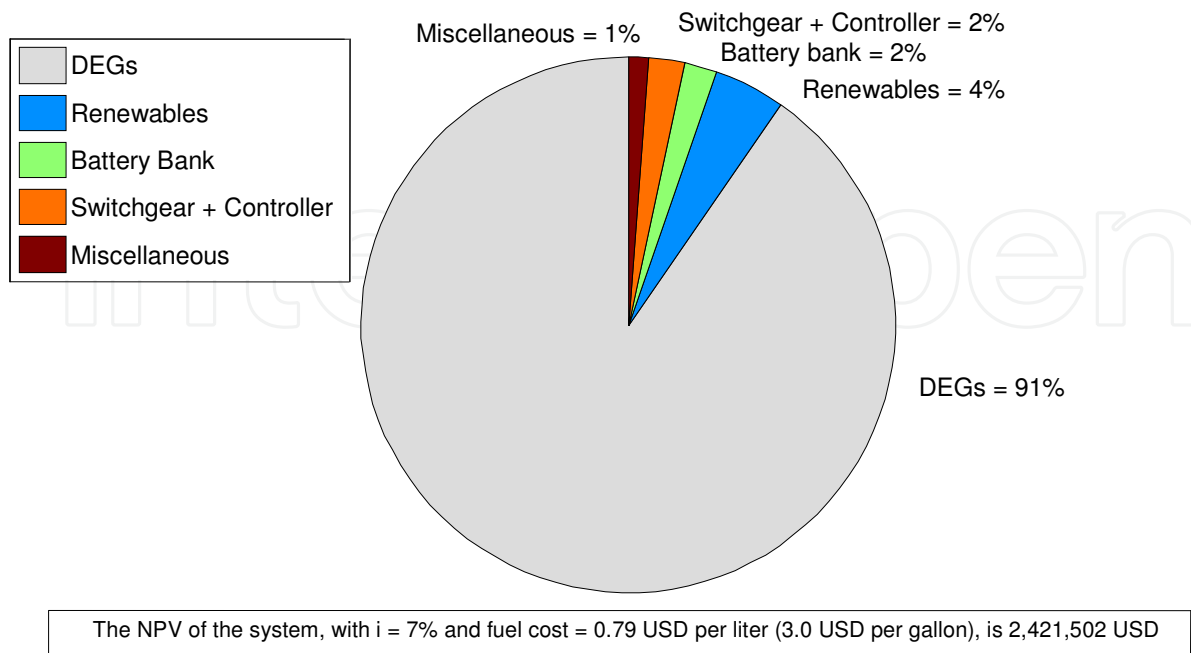


Fig. 12. 20-year LCC analysis of the hybrid power system using HOMER.

power source used in HOMER. Therefore, the life of the battery bank is less in HARPSim due to the annual increase in charge/discharge cycles. This results in more efficient operation of the DEGs while reducing the fuel consumption and saving in the cost of the DEGs. Overall, the LCC analysis shows a lower NPV in HARPSim than in HOMER.

#### 4.4 Sensitivity analysis: Fuel cost on NPV, cost of energy, and payback period

The plot for sensitivity analysis of fuel costs and investment rate on the NPV for the PV-wind-diesel-battery system is shown in Fig. 13. It can be seen that as the cost of fuel increases and the investment rate decreases, the NPV of the system increases. The NPV plays an important role in deciding on the type of the system to be installed. The NPV of a system includes the total spending on the installation, maintenance, replacement, and fuel cost for the type of system over the life-cycle of the project. Knowing the NPV for different system configurations, the user can install a system with minimum NPV.

The plot for sensitivity analysis of fuel costs and investment rate on the COE for the PV-wind-diesel-battery system is shown in Fig. 14. It can be observed that as the cost of fuel increases and the investment rate increases, the COE increases.

In order to calculate the COE for the diesel-battery (high emissions plant) system and the PV-wind-diesel-battery (low emissions plant) system, it is necessary to know the A/P ratio for the system, where 'A' is the annual payment on a loan whose principal is 'P' at an interest rate 'i' for a given period of 'n' years (Sandia, 1995).

The ratio A/P is given as follows:

$$\frac{A}{P} = \frac{i(1+i)^n}{(1+i)^n - 1} \tag{17}$$

The annual COE for different systems given a fuel price in USD per liter (4.00 USD per gallon) and an investment rate (%) is calculated as follows:

$$COE_L = \left(\frac{A}{P}\right)_L (C_{PV-wind} - C_{DB}) + \left(\frac{A}{P}\right)_H (C_{DB}) + C_F \tag{18}$$

and

$$COE_H = \left(\frac{A}{P}\right)_H (C_{DB}) + C_F, \tag{19}$$

where  $C_{PV-wind}$  is the cost of the PV-wind-diesel-battery system from Table 2,  $C_{DB}$  is the cost of the diesel-battery system from Table 2 and  $C_F$  is the annual cost of fuel from Table 3.

The plot for sensitivity analysis of fuel costs and investment rate on the payback period for the PV-wind-diesel-battery system is shown in Fig. 15. It can be seen that the payback period of the PV array decreases as a function of a fifth order polynomial with the increase in the cost of fuel.

The simple payback period (SPBT) for the PV array and WTG is calculated using data from Table 2 and Table 3 as

$$SPBT = \frac{\text{Extra cost of PV system}}{\text{rate of saving per year}} \tag{20}$$

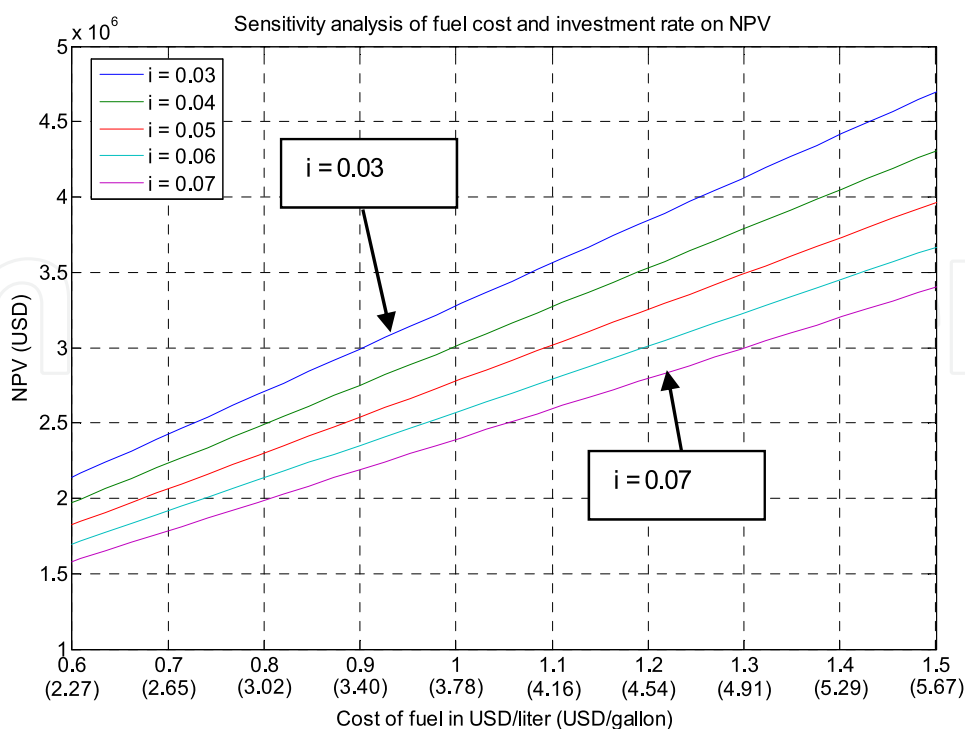


Fig. 13. Sensitivity analysis of fuel cost and investment rate on the NPV.

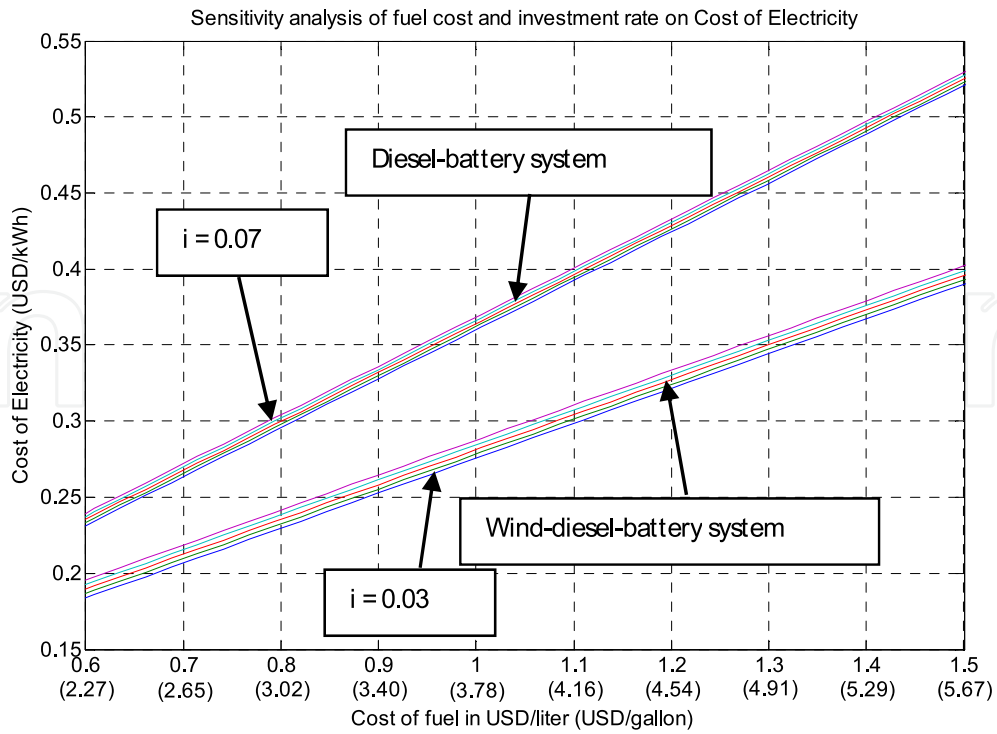


Fig. 14. Sensitivity analysis of fuel cost and investment rate on the COE.

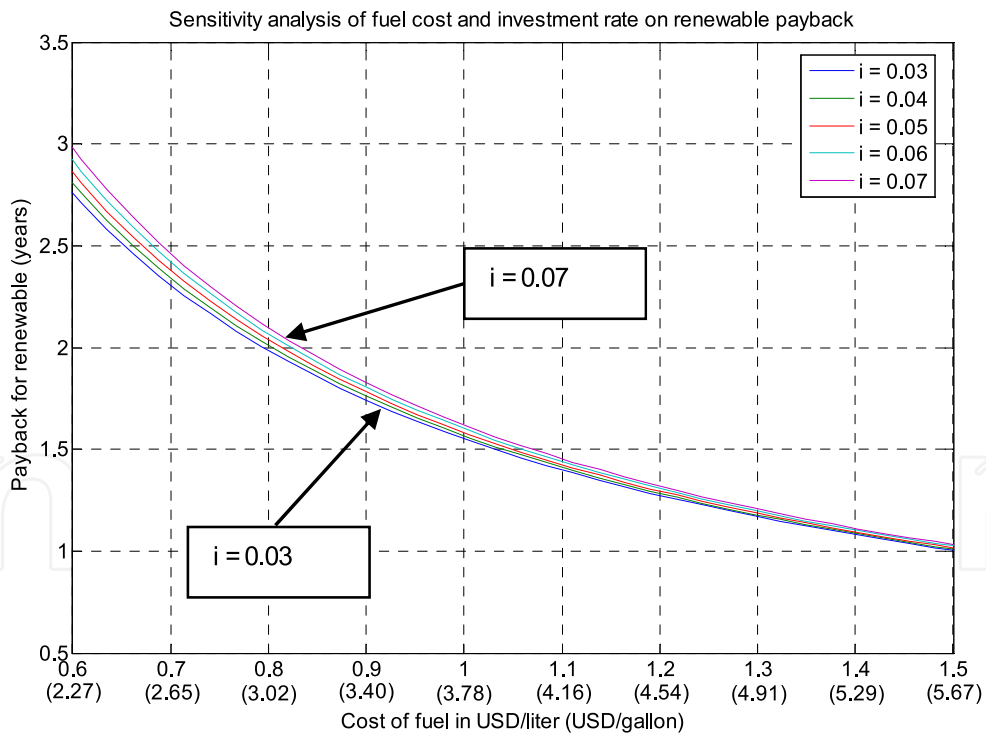


Fig. 15. Sensitivity analysis of fuel cost and investment rate on the payback period.

The extra cost of the PV array and WTG in the system is obtained as the difference between the system cost of the PV-wind-diesel-battery system and the diesel-battery system from Table 2 and the rate of savings per year is obtained from the savings in the cost of fuel per year as given in Table 3.

## 5. Conclusion

A model called HARPSim was developed in MATLAB® Simulink® to demonstrate that the integration of WTGs and PV arrays into stand-alone hybrid electric power systems using DEGs in remote arctic villages improves the overall performance of the system. Improved performance results from increasing the overall electrical efficiency, while reducing the total fuel consumption of the DEG, the energy costs, and emissions.

The LCC cost analysis and the percentage annualized cost from the Simulink® model were comparable to those predicted by HOMER. The Simulink® model calculates the CO<sub>2</sub>, NO<sub>x</sub> and the PM<sub>10</sub> emitted to the atmosphere over the period of one year. These results can also be utilized to calculate the avoided costs of emissions.

Distributed or hybrid energy systems which result in more economical and efficient generation of electrical energy could not only improve the lifetime and reliability of the diesel-electric generation systems in remote communities, but could also help to extend the future of non-renewable energy sources.

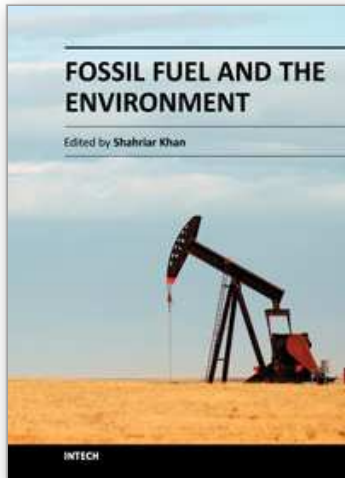
## 6. Acknowledgment

The authors would like to thank Peter Crimp of the Alaska Energy Authority and Dennis Meiners of Intelligent Energy Systems for providing the power system information and data for the sample village electric power system. The authors would also like to thank Siemens, Entegri Wind Systems (formerly Atlantic Orient Corporation), Caterpillar (Detroit Diesel) and GNB Industrial for providing the design specifications for the PV panels, wind turbines, diesel-electric generator and battery bank, respectively.

## 7. References

- Agrawal, A. (2006). "Hybrid Electric Power Systems in Remote Villages: Economic and Environmental Analysis for Monitoring, Optimization, and Control," *Ph.D. Dissertation*, Dept. of Elect. and Comp. Eng., Univ. of Alaska, Fairbanks.
- Atlantic Orient 15/50 Brochure (2005). *Official Website of Atlantic Orient Canada Inc.*, accessed Aug 8<sup>th</sup>, 2011, Available from: <http://www.atlanticorientcanada.ca/pdfs/AOCI-SalesSheet2005-1.pdf>.
- Borowy, B. (1996). "Design and Performance of a Stand Alone Wind/Photovoltaic Hybrid System," *Ph.D. Dissertation*, Dept. of Elect. Eng., Univ. of Massachusetts, Lowell.
- Cengel, Y. & Boles, M. (2002). "Engineering Thermodynamics", *McGraw Hill Publications*, 4<sup>th</sup> ed.
- Dawson, F. & Dewan, S. (September 1989). "Remote Diesel Generator with Photovoltaic Cogeneration", *Solar'89*, pp. 269-274.
- Denali Commission (August 2003). Memorandum of Agreement Re Sustainability of Rural Power Systems, *A Memorandum of Agreement between the Denali Commission, the Alaska Energy Authority and the Regulatory Commission of Alaska*, August 2003.
- Drouilhet, S. & Shirazi, M. (September 1997) "Performance and Economic Analysis of the Addition of Wind Power to the Diesel Electric Generating Plant at Wales, Alaska", *a report prepared by the National Renewable Energy Laboratory*.

- US Energy Consumption Database (2002). *US Department of Energy Energy Information Authority Website*, accessed on July 9, 2002, Available from: <http://www.eia.doe.gov/emeu/sep/ak/frame.html>.
- Fyfe, W.; Powell, M., Hart, B. & Ratanasthien, B. (1993) "A Global Crisis: Energy in the Future", *Nonrenewable Resources*, pp. 187-195.
- HOMER Software, *Official Website of the National Renewable Energy Laboratory*, accessed August 8<sup>th</sup>, 2007, Available from: <http://www.nrel.gov/homer/>.
- Johansson, T.; Kelly, H., Reddy, A. & Williams, R. (1993). *Renewable Energy Sources for Fuels and Electricity*, Island Press, Washington, D.C.
- Malosh, J. & Johnson, R. (June 1985). "Part-Load Economy of Diesel-Electric Generators", *a report prepared for Department of Transportation and Public Facilities*, report # AK-RD-86-01.
- NREL GIS Solar Data and Maps (2007). *Official Website of the National Renewable Energy Laboratory*, accessed August 8<sup>th</sup>, 2011, Available from: <http://www.nrel.gov/gis/solar.html>.
- NREL Solar Radiation Resource Information (2007). *Official Website of National Renewable Energy Laboratory Renewable Resource Data Center*, accessed August 8<sup>th</sup>, 2011, Available from: <http://rredc.nrel.gov/solar>.
- Patel, M. (1999). "Wind and Solar Power Systems", *Florida: CRC Press LLC*, 1<sup>st</sup> ed.
- Sandia National Laboratories (March 1995). "Stand-Alone Photovoltaic Systems - A Handbook of Recommended Design Practices", *a report prepared by Sandia National Laboratories*, report # SAND87-7023.
- Wies, R.; Johnson, R., Agrawal, A. & Chubb, T. (2005a). "Simulink Model for Economic Analysis and Environmental Impacts of a PV with Diesel-Battery System for Remote Villages," *IEEE Transactions on Power Systems*, vol. 20, no. 2, pp. 692-700.
- Wies, R.; Agrawal, A. & Chubb, T. (2005b). "Optimization of a PV with Diesel-Battery System for Remote Villages," *International Energy Journal*, vol. 6, no.1, part 3, pp. 107-118.
- Wies, R.; Johnson, R. & Agrawal, A. (2005c). "Life Cycle Cost Analysis and Environmental Impacts of Integrating Wind-Turbine Generators (WTGs) into Standalone Hybrid Power Systems," *WSEAS Transaction on Systems*, iss. 9, vol. 4, pp. 1383-1393.
- Winsor, W. & Butt, K. (September 1978). "Selection of Battery Power Supplies for Cold Temperature Application", *Technical report, C-CORE Publication No. 78-13*.



## **Fossil Fuel and the Environment**

Edited by Dr. Shahriar Khan

ISBN 978-953-51-0277-9

Hard cover, 304 pages

**Publisher** InTech

**Published online** 14, March, 2012

**Published in print edition** March, 2012

The world today is at crossroads in terms of energy, as fossil fuel continues to shape global geopolitics. Alternative energy has become rapidly feasible, with thousands of wind-turbines emerging in the landscapes of the US and Europe. Solar energy and bio-fuels have found similarly wide applications. This book is a compilation of 13 chapters. The topics move mostly seamlessly from fuel combustion and coexistence with renewable energy, to the environment, and finally to the economics of energy, and food security. The research and vision defines much of the range of our scientific knowledge on the subject and is a driving force for the future. Whether feasible or futuristic, this book is a great read for researchers, practitioners, or just about anyone with an enquiring mind on this subject.

### **How to reference**

In order to correctly reference this scholarly work, feel free to copy and paste the following:

R. W. Wies, R. A. Johnson and A. N. Agrawal (2012). Energy-Efficient Standalone Fossil-Fuel Based Hybrid Power Systems Employing Renewable Energy Sources, Fossil Fuel and the Environment, Dr. Shahriar Khan (Ed.), ISBN: 978-953-51-0277-9, InTech, Available from: <http://www.intechopen.com/books/fossil-fuel-and-the-environment/energy-efficient-standalone-fossil-fuel-based-micro-grid-systems-with-renewable-energy-and-smart-gri>

**INTECH**  
open science | open minds

### **InTech Europe**

University Campus STeP Ri  
Slavka Krautzeka 83/A  
51000 Rijeka, Croatia  
Phone: +385 (51) 770 447  
Fax: +385 (51) 686 166  
[www.intechopen.com](http://www.intechopen.com)

### **InTech China**

Unit 405, Office Block, Hotel Equatorial Shanghai  
No.65, Yan An Road (West), Shanghai, 200040, China  
中国上海市延安西路65号上海国际贵都大饭店办公楼405单元  
Phone: +86-21-62489820  
Fax: +86-21-62489821

© 2012 The Author(s). Licensee IntechOpen. This is an open access article distributed under the terms of the [Creative Commons Attribution 3.0 License](#), which permits unrestricted use, distribution, and reproduction in any medium, provided the original work is properly cited.

IntechOpen

IntechOpen